Installation for Biomagnetic Researches

Octavian Baltag[1], Doina Costandache[2], Miuta Carmina Rau[3]

Medical Bioengineering Department, University of Medicine and Pharmacy "Grigore T. Popa" - Iasi
No. 16 Iasi, Universitatii Street, Romania

[1]octavian.baltag@bioinginerie.ro; [2]costandache_doina@yahoo.com; [3]miuta.carmina@gmail.com

***Abstract*-The paper presents a complex installation destined to biomagnetic researches. The structure of the installation consisting of a shielded aluminum room, coil systems for the control of the surrounding magnetic field components and a SQUID HTS gradiometer is described. The performances of the realized installations allowed us to register for the first time in Romania a biomagnetic signal generated by the cardiac activity.**

Keywords-Biomagnetometry; Biomagnetism; Helmholtz Coils; Active Compensation; Shielded Room

I. INTRODUCTION

Unlike the classic magnetometry, the biomagnetometry requires special conditions to carry out magnetic field measurements. Generally, these conditions are determined by two factors:

- the low level of the biomagnetic field produced by the bioelectric activity, as well as by the presence of some acquired magnetic elements;

- the interference with natural magnetic field, as well as with the fields produced by human activity.

Taking the geomagnetic field ($5x10^{-5}$ T) as reference, a biomagnetic field of 100 fT (10^{-13} T) results in an unfavorable signal to noise ratio (10^{-8}). Due to this, the biomagnetic installations can only work under special electromagnetic environmental conditions; these refer to the diminution of the environmental field down to levels comparable to biomagnetic signals. Shielded rooms and coil systems are used for this aim. Another solution to improve the signal to noise ration consists in measuring the biomagnetic field gradients. This solution is applied both in the case of complex installations that use shielded spaces, and in unshielded environments. In order to provide an electromagnetic medium where the residual magnetic field is lower than 1 nT, one can use in principle the following methods:

- magnetic shields executed from walls made of high permeability ferromagnetic materials [1], [2], [3], [4];

- compensation coils having the size corresponding to the volume where the measurements are carried out [5], [6];

- active compensation coils by whose means the local variations of the environmental field are controlled [7], [8], these systems make use of a negative reaction loop which provides an automated control of the variable environmental field compensation;

- complex systems consisting of shielded rooms of ferromagnetic and/or non-ferromagnetic materials, together with large size coil systems which perform the static and dynamic control of the magnetic field level [9], [10].

The utilized SQUID biomagnetometer is located in the center of the room and of the control coils, within the space where the lowest level of the field and the residual gradients is assured. The subject or the object investigated is placed in the same volume on a support that can be moved in a triaxial or cylindrical coordinate system accordingly.

Table I presents a synthesis of the active and passive shielding methods used for the compensation and control of the environmental magnetic fields.

TABLE I CLASSIFICATION OF THE MAGNETIC SHIELDING METHODS

Materials	Combination	Compensation	Applications
Ferromagnetic with High Magnetic Permeability-Mumetal, Permalloy, Fe-Si Alloy	Cube or Parallelepiped Shape with 1, 2, 3, 6 or 8 Layers with Uniaxial or Triaxial Coils System and Negative Feedback Assembly	For Passive and Active Shielding	Based on High Magnetic Permeability of Permalloy, for ELF Shielding
Non-ferromagnetic (Al, Cu) Materials with High Electric Conductivity	Walls with 1, 2, 3 Layers and Uniaxial or Triaxial Coils System and Negative Feedback Assembly	For Passive and Active Shielding	Based on Lenz Law, for EHF Shielding
Ferromagnetic and Non-ferromagnetic	Sandwich Type with Air, Wood, Plastic, Glass in Combination, Permalloy with Al or Cu and with Uniaxial / Triaxial System Coils and Negative Feedback Assembly	Passive and Active Shielding	Biomagnetism, Satellites, Generally Equipment Using Electron Guns or Ions Sources and Mass Spectrometry, Masers and Atomic Clocks, Electron Microscopy and Transmission Electron Microscopy, SEM (Scanning Electron Microscopy), SQ UID, MRI, Electron Beam Instruments

The biomagnetic measurements use the SQUID systems of magnetometers / field gradiometers type, with a number of channels according to the investigation. In some research applications, fluxgate transducers [11], [12], GMR [13], and optical pumping are used [14]. A special perspective can have the optic pumping magnetometer with sub-fT performances [15].

The magnetic fields that can be detected and measured at a living organism have different natures. Some are produced by the electric activity of the living organism, other result from the accumulation of metallic deposits (iron), due to pathological metabolic processes (iron accumulations in spleen, liver, heart etc), or to occupational diseases (silicosis) in some specific activities (miners, welders, metallurgists etc).

TABLE II
BIOMAGNETIC MEASUREMENTS

Organ Studied	Method Signal Intensity Signal Frequency	Principle or Type	Clinic Implementations	Electric Analogue Method
Heart	MCG -Magnetocardiography, (1- 100) pT (0,01- 100) Hz	SQUID Functional Imaging	Usual Clinical	ECG, Electrocardiography
Heart	Vectormagnetocardiography	Clinical Research	Clinical Research	Vectorcardiography
Brain	MEG – Magnetoencefalography (1-10) pT, (0,1-100) Hz	Squid Functional Imaging	Usual Clinical	EEG Electroencefalography
Brain	Quasistatic Magnetometry (MEG Extension to Very Low Signal Frequency) (0,1-10) pT / (10^{-3}- 1) Hz	MEG with Mechanical Modulation	Research	None Practical
Brain	Auditory Evoked Responses Provoked by Pain, in Adult 400 fT	Functional Imaging	Research	Evoked Potentials
Nervous System	MNG-Magnetoneurography (10^{-3}- 10^{-2}) pT (10^{2}- 10^{3}) Hz	Neural Stimulated Impulses & Mapping	Research	-
Peripheral Nervous System	Axon Magnetic Field	Neural Stimulated Impulses	Research	-
Stomach	MGG – Magnetogastro-graphy (1 – 20) pT / 0,05 Hz	Stomach Magnetic Activity	Research	EGG Electrogastrogram
Intestine	MENG – Magnetoente-rography (0,1 – 10) pT (0,01 – 0,05) Hz	Mapping	Research	-
Pancreas	MPG – Magnetopancreatogram	Research Hypotesis	Research Hypotesis	-
Multiple Organs	LFMRI – Low Field Magnetic Resonance Imaging fT – pT, 10^3 Hz	Structural Imaging	Research	-
Muscles	MMG Magnetomiography	Muscular Activity	Research	Electromiography
Blood	Citomagnetometry	Research Hypotesis	Research Hypotesis	None
Foetus	fMCG–Fetalmagneto-Cardiography (0,5 – 10) pT	Functional Imaging	Clinical Practice	fECG Invasive Method
Foetus	fMEG – Fetalmagneto-Encefalography, 100 fT	Functional Imaging	Research	-
Foetus	fAERs, Fetal Auditory Evoked Responses Magnetic Fields (10 – 100) fT	Clinical Research	Research Clinical Practice	Evoked Potentials
Foetus	fVERs - Fetal Visual Evoked Responses Magnetic Fields (fT)	Research Hypotesis	-	Evoked Potentials
Foetus	fPERs - Fetal Pain Evoked Responses Magnetic Fields (fT)	Research Hypotesis	-	Evoked Potentials
Uterus	Benign Formations in Uterine Wall	Research Hypotesis	-	-
Uterus	Utero - Placentar Hemodynamics	Clinical Research	-	-
Ovarus	Malignant or Benign Formations at the Ovaries (fT)	Clinical Research	-	-
Prostate	Malignant Formations in Cancer Prostate	Clinical Research	-	-

Table II presents a synthesis of the biomagnetic fields measurements due to the electric activity of living tissues and organs [16], [17], [18], [19], [20], [21].

Table III presents a synthesis of the biomagnetic fields measurements produced by accumulation and generation of ferromagnetic deposits in various organs as the result of some metabolic phenomena, performing specific jobs – occupational diseases, or investigation with magnetic tracers [22], [23], [24], [25].

TABLE III
BIOMAGNETIC FIELDS PRODUCED BY FERROMAGNETIC DEPOSITS

Organ	Method Signal Intensity	Principle	Clinic Implementation
Lungs	MPG Magnetopneumography, (10^2 – 10^3) pT (0,1 – 10) Hz	Magnetic Impurities Fluxgate & SQUID	Research No Clinical Use
Liver	Liver Susceptometry (0,1 – 10) pT , 10 Hz	Susceptometry	Clinical Practice
Heart	Iron Deposit in Heart	Susceptometry	Research
Breast Cancer	In Vivo Immunoassay (10^{-2} – 10) pT (0,1 – 1) Hz	Magnetic Label Detection	Research
Breast Cancer	Mmamg – Magneto-Mammography	Structural Imaging	Research Hypotesis
Orocecal Transition	SQUID	Magnetic Markers	Research

II. DESCRIPTION OF THE INSTALLATION

The magnetometric installation is a mixed system consisting of:

- shielded room of nonferromagnetic material;
- a triaxial Helmholtz coil system for the compensation of continuous components of the local geomagnetic field;
- a triaxial Helmholtz coil system for the compensation of variable components of the geomagnetic fields or those produced by human activity;
- triaxial magnetometer for variable magnetic field control;
- HTS SQUID biomagnetometer.

The installation is located in the building of the Faculty of Medical Bioengineering, at the ground floor. Its geographic coordinates are: $47^0$10’25”N longitude, $27^0$35’19”E latitude [26], altitude: 240 m. The magnetic field values are: total component: 49,102.5 nT, horizontal component: 21,294.6 nT, vertical component: 44,244.7 nT, East-West component: 2094.2 nT, North-South component: 21,191.4 nT, Declination: $5^0 30'$, Inclination: $64^0 18'$ [27]. The shielded room and the square Helmholtz coils system are in line with one of the axis parallel to the local magnetic meridian.

The shielded room [28] provides the shielding against the environmental magnetic field. This has a parallelepiped shape sized (3 x 2 x 2) m. It consists of 0.012 m thick aluminum walls and is placed on a wood support, in the centre of the Helmholtz system. Aluminum was used for reasons of cost, construction easiness, and because it does not modify the spectrum of the magnetic field produced by the coils inside it. The room walls are coated with absorbing material within the range of very high frequencies, forming thus an anechoic structure. The absorbing material is of polyurethane pyramidal foam with carbon powder. The room shielding coefficients differ along the three coordinates due to the parallelepiped configuration, Fig. 1.

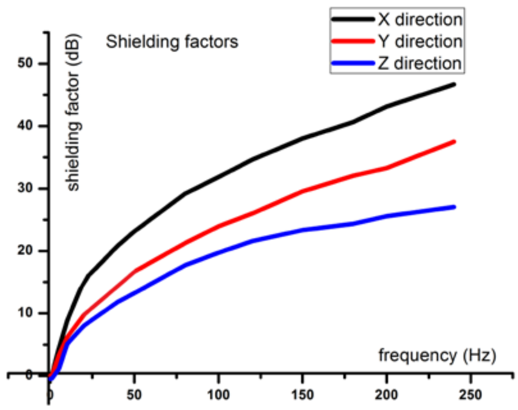

Fig. 1 Shielding factors along the three directions

The triaxial Helmholtz coil systems are executed on a skeleton made of wood dimensionally stabilized by long lasting treatment. Each pair of coils includes two winding groups: one destined to the manual compensation of the geomagnetic continuous field component, and the other used to compensate for the alternative variable components.

The ratio of the constants of the two coils is 1/5. The currents flowing through the coils for the continuous component compensation are applied from voltage controlled current sources. The block diagram of this system is presented in Fig. 2.

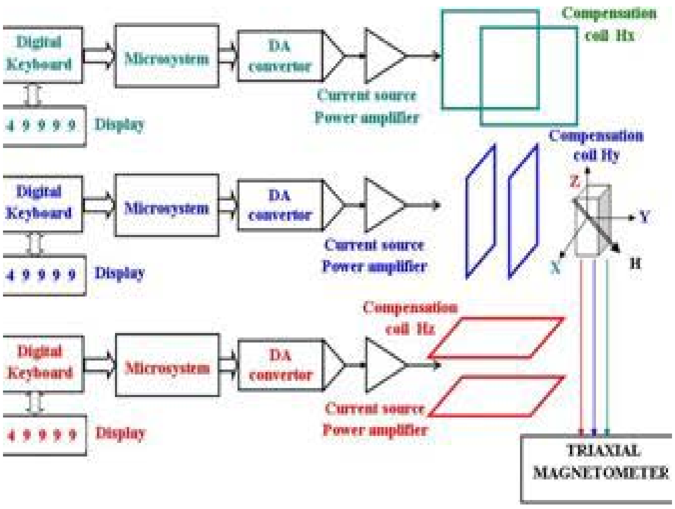

Fig. 2 The block diagram of the manual compensation system

The control voltages of the current sources can be analogically applied through a helicoidally or digital potentiometer, by means of a keyboard. The current constants of the three compensation coils are: K_x=0.6093x10^{-4}T/A; K_y=0.6292x10^{-4}T/A; K_z=0.4875x10^{-4} T/A. The external field compensation level is permanently measured by means of a triaxial magnetometer. This system is independent from the rest of the installation and is only used to reduce the geomagnetic field intensity. The compensation is carried out independently on the three channels galvanic separated down to a preestablished value. The compensation range for the three directions is of +/- 50,000 nT. The compensation precision depends on the field measurement precision. The residual field includes variable and alternative components due to geomagnetic field natural variation, to human activity and to electric network frequency of 50 Hz. The block diagram of the control system for the variable and alternative fields is presented in Fig. 3.

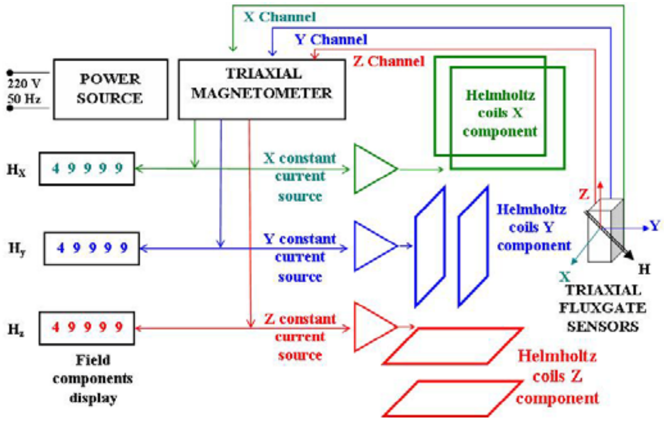

Fig. 3 The block diagram of the automatic compensation system

These coils work in a negative feedback loop together with a triaxial magnetometer and the voltage controlled current sources. The triaxial magnetometer supplies the control voltage for the current sources. The currents injected in the Helmholtz coils generate a resulting field in opposition with the disturbing field. The current constant of these coils is 5 times lower than that of compensation coils, namely: k_x=0.1218x10^{-4} T/A; k_y=0.1258x10^{-4} T/A; k_z=0.0975x10^{-4} T/A.

In the realized installation, a triaxial HTS SQUID biomagnetometer was used, delivered by Tristan Company, USA, which is not destined to gradient measurement. This was converted into a 1st and 2nd order SQUID gradiometer system to measure the vertical component of the magnetic field gradient. The magnetometer sensors are connected such that to get three channels for the 1st order gradient and one channel for the 2nd order gradient, with electronic subtraction, Fig.4 [29].

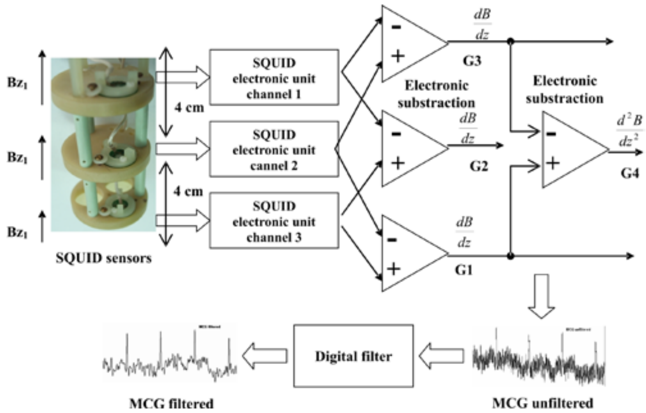

Fig. 4 First and second order gradiometers system

The adopted solution is advantageous due to the fact that, from the three SQUID magnetometer channels, one can make several SQUID gradiometers, using the electronic subtraction of the signal arriving from the three individual magnetometer channels. At first, the three magnetometer channels were fixed in a triaxial holder which permitted the control of the three components of the biomagnetic field. In order to improve the signal/noise ratio, the three channels were converted into gradiometers. For gradient measurement, the SQUID sensors were moved from their initial position in three coaxial holders placed vertically. The distance to the neighboring sensors is 4 cm and represents the baseline of gradiometer. The distance between the extreme - proximal and distal - sensors is of 8 cm. This gradiometers differ from the classical ones accomplished with sensors (superconducting coils) connected in opposition.

The three magnetometer channels are galvanic separated from each other. They transmit the analogue signal to a conversion circuit which communicates at distance with the electronic blocks through optical cable. The optical interface communicates with digital/analog conversion circuits and delivers an analogic signal proportional to the measured field.

This configuration permits the realization of the following gradiometer structure:

- a 1st order gradiometer consisting of the proximal and middle sensor, with a 4 cm baseline;
- a 1st order gradiometer accomplished between the middle and distal sensors, with a 4 cm baseline;
- a 1st order gradiometer realized between the extreme, proximal and distal sensors, with 8 cm baseline;
- a 2nd order gradiometer with a 4 cm baseline, realized through electronic subtraction procedure of the signals recorded from the first two 1st order gradiometers.

As the three magnetometer channels have different sensitivities, in order to carry out the electronic subtraction, electronic circuits were introduced which perform the leveling of factors or transfer coefficients (channels sensitivity). For gradiometer channels adjustment, we used the following procedure: using a Helmholtz generator of magnetic field, one applies to each channel a known field, and the individual amplification factor is adjusted until the sensitivity of the three channels is the same.

The signals coming from the three magnetometer channels are applied at the analogue subtraction circuits executed with operational amplifiers. At the output of the analogue circuits signals are obtained proportional with the magnetic field gradient, determined by the intensity of the fields at the level of the three SQUID sensors of the magnetometer channels. The thus realized SQUID gradiometers are installed in the centre of the shielded rooms and of the Helmholtz system, above a bed with horizontal mobility.

III. THEORETICAL BASIS OF NEGATIVE FEEDBACK

The operation of a compensation system using the negative feedback is presented in Fig. 5.

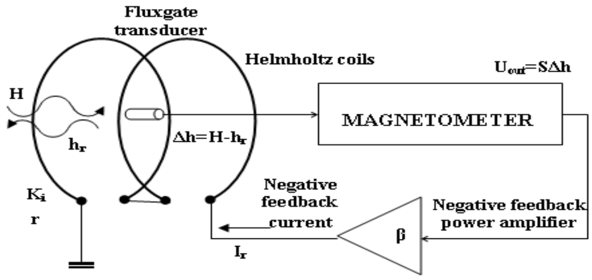

Fig. 5 Negative feedback system

Such a system consists of the following elements: vector magnetometer located inside the coil system, power amplifier and coil system.

The following notations are used: B_0 – environmental magnetic field; U_{out}– output voltage of the magnetometer with open negative feedback loop; β – amplification factor of the negative feedback loop; K_i – current constant of the automated compensation winding; r – resistance of the compensation winding, S – transfer function of the magnetometer, U_{out} – output voltage of the magnetometer with active negative feedback loop. The environmental magnetic field B_0 is compensated by the triaxial components of the compensating field B generated by the Helmholtz coils. The value of this field results from the relation which describes the negative feedback loop from Fig. 5:

$$B = K_i I_r = K_i \frac{U_{out}\beta}{r} = K_i \frac{S}{r}\beta(B_0 - B) = \alpha(B_0 - B) \quad (1)$$

where we used the notation:

$$\alpha = K_i S\beta/r \ . \quad (2)$$

The residual field has the value:

$$\Delta B = B_0 - B = \frac{B}{\alpha} \quad (3)$$

From the relation (3) it follows that the compensation efficiency $\Delta B/B_0$ depends on the factor α:

$$\frac{\Delta B}{B} = \frac{1}{\alpha} \quad (4)$$

In order to obtain an efficient compensation, the condition $\frac{\Delta B}{B} << 1$ must be satisfied, which leads to the relation $\alpha >>1$.

This relation gives the conditions necessary for the system to accomplish the compensation: S – high sensitivity of the magnetometer, high gain factor for the negative feedback loop $\beta>>1$, current constant K_i as high as possible, compensation winding resistance as small as possible.

The negative feedback extends the qualities of accuracy and time stability over the properties and gain of the entire system. In order to determine the effect of the factors of influence on the automated compensation system, the derivatives of relation (4) in terms of the parameters S, β, Ki and r are analysed.

$$\frac{d}{dK_i}\left(\frac{\Delta B}{B}\right) = -\frac{1}{K_i}\frac{r}{K_i S\beta} \quad (5)$$

$$\frac{d}{dS}\left(\frac{\Delta B}{B}\right) = -\frac{1}{S}\frac{r}{K_i S\beta} \quad (6)$$

$$\frac{d}{d\beta}\left(\frac{\Delta B}{B}\right) = -\frac{1}{\beta}\frac{r}{K_i S\beta} \quad (7)$$

$$\frac{d}{dr}\left(\frac{\Delta B}{B}\right) = \frac{1}{r}\frac{r}{K_i S\beta} \quad (8)$$

From relations (5), (6), (7) and (8), one can notice that the dependence of the error signal on the coefficients S, β, Ki and r which can change due to some influential factors, is reduced by a factor of $1/\alpha$ due to the negative feedback [30].

IV. EXPERIMENTAL RESULTS

The dimensions of the magnetometric installation are presented in Fig. 6.

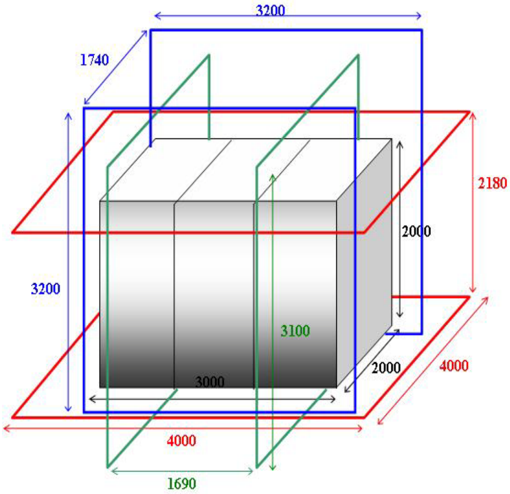

Fig. 6 The dimensions of the Helmholtz coil system and the shielded room

The shielded room and the triaxial Helmholtz coil system, together with electronic block which controls the compensating currents, biomagnetic data acquisition system are presented in Fig. 7.

Fig. 7 Shielded room, Helmholtz coil system and the electronic control block

Fig. 8 presents the inside of the room together with the SQUID gradiometer and the mobile bed.

Fig. 8 Inside the shielded room

In order to carry out measurements meant to record a magnetocardiogram, the following operations were executed:

- diminish the geomagnetic field down to the level of some nanotesla, by injecting currents in the triaxial Helmholtz system;
- activate the system for automated compensation of the variable magnetic field through negative feedback;
- calibrate the SQUID gradientmeter using a standard Helmholtz coil as a field and gradient generator.

The subject is lying in supine position on the mobile bed, with the SQUID gradientmeter fixed over the subject's thorax; the gradientmeter's sensor, which is situated in its lowest part, is located at a distance of 2 cm from the thorax. Simultaneously with magnetocardiogram recording, an electrocardiogram was executed, with standard derivations. The utilized electrodes are non-magnetic. The magnetograms were measured over regions which correspond to the anatomical landmarks of the chest: the 5th left intercostal space, on the mid-clavicular line and in the xiphoid process zone. Fig. 9 presents a magnetocardiogram and an electrocardiogram, simultaneously recorded, from an adult subject of 66 years old, without pathological cardiac antecedents.

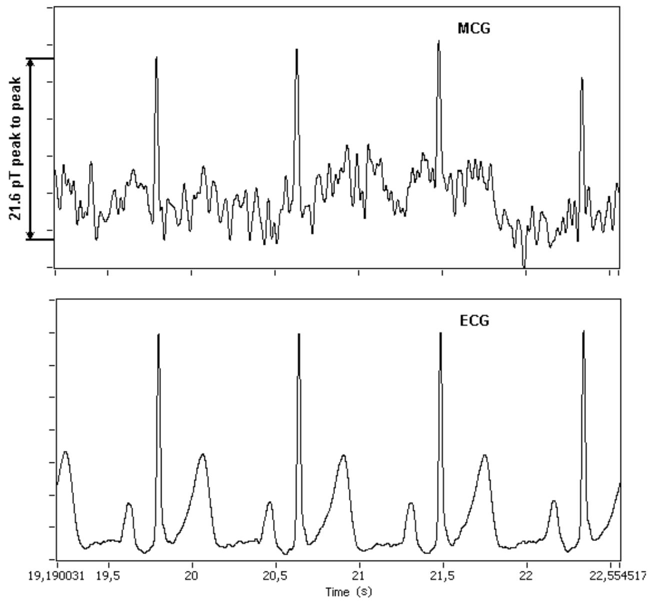

Fig. 9 Magnetocardiogram and electrocardiogram

For this recording, the sensor was positioned over the lower region of the thorax, in front of the xiphoid process, with the specification that the subject was in apnoea after forced inspiration. This region was chosen because the component of the magnetic field produced by the cardiac dipole, perpendicular to the thorax, has the largest value. The thorax motions during breathing can determine the shift of the position of the heart magnetic moment through the spatial displacement of the heart inside the thorax; this shift of the heart magnetic moment determines the modulation of the MCG signal. For this reason, the patient presented an episode of controlled apnoea during recording.

The recording was carried out opposite to the right xiphoid process in apnoea condition. The gradient of the measured field has the value of 21.6 pT_{pp}. The noise level is of 10 pT_{pp}. The noise spectrum contains both even and odd harmonics of the mains frequency: 100 Hz and 150 Hz. The gradientmeter frequency band is DC ÷ 5000 Hz. The signal level at the gradientmeter output was of 21, 6 pT_{pp}. In order to record the magnetocardiogram, an electronic filter was used with the bandwidth of (0.05–38) Hz. On the filtered magnetocardiogram, one can notice the existence of the QRS complex, as well as of the P and T waves corresponding to a standard electrocardiogram. One can notice the temporal coincidence of these signals. The filtered magnetocardiogram is presented in Fig. 9 [31]. In order to improve the magnetocardiogram recording and interpretation, electronic data processing is recommended, using programs like ICA or Wavelet.

V. CONCLUSIONS

The realized installation allows performing biomagnetic field measurements. The shielded room accomplishes the shielding of medium and high frequency electromagnetic fields.

The environmental magnetic fields diminished to levels on which the operation of SQUID magnetometer is ensured by using static and dynamic compensation method.

The control system for the subject movement in horizontal level permits to set out biomagnetic field maps.

The magnetogram recording was possible by the realization of a complex biomagnetometric installation which provides environmental conditions necessary to the operation of the SQUID gradiometer.

The recorded magnetocardiographic signal corresponds to the ECG signal from both morphologic and temporal points of view.

REFERENCES

[1] G. Kajiwara, K. Harakawa and H. Ogata, "High performance magnetically shielded room", *IEEE Trans.on Mag.*, vol.32, pp. 2582-2585, 1996.

[2] K. Harakawa, G. Kajiwara, K., Kazami, H. Ogata, H. Kado, "Evaluation of a high performance magnetically shielded room for biomagnetic measurement", *IEEE Trans.on Mag.*, vol.32, pp.5226-5259, 1996.

[3] D. Cohen, U. Schlapfer, S. Ahlfors, et all, "New six layer magnetically shielded room for MEG", *Proc. of the13th Int. Conf.on Biomagnetism, Jena, Germany*, 2002.

[4] J. Bork, H.D. Hahlbohm, R. Klein, A. Schnabel, "The 8 layered magnetically shielded room of PTB: design and construction", *Proc. 12th Int. Conf. on Biomagnetism*, 2000, Espoo, Finland, pp. 970-973, 2000.

[5] O. Baltag, "Dynamic control and annulement of electromagnetic pollution", in *Proc. 11th Int. Symposion of EMC*, Zurich, pp. 75L6, l995.

[6] T. Brys, S. Czekaj, M. Daum, et all., "Magnetic field stabilization for magnetically shielded volumes by external field coils", *Jour. Res. Natl. Inst. Stand. Technol*, vol 110, pp. 173-178, 2005.

[7] D. Platzek, H. Nowak, F. Giessler, J. Rother and M.Eiselt, "Active shielding to reduce low frequency disturbances in direct current near biomagnetic measurements", *Rev. Sci.Instrum.*, vol. 70, pp.2465-2470, 1999.

[8] O. Baltag, D. Costandache, "Dynamic control and annulment of electromagnetic pollution" in *Proc. IMEKO TC19 2007*, pp. 119-121, 2007.

[9] K. Kato, K. Yamazaki, H. Matsuba, C. Sumi and S. Sato, "Active magnetic shield for biomagnetic measurement", in Proc. *Int. Conf. on Biomagnetism, 2000*, Espoo, Finland, pp. 965-967, 2000.

[10] O. Baltag, D. Costandache, M. Rau, A. Iftemie, I. Rau, "Dynamic shielding of the magnetic fields" *Advances in Electrical and Computer Engineering*, vol. 10, pp. 135-140, 2010.

[11] I. Platil, P. Ripka, P. Kaspar, A. Tipek, K. Svabova and R. Holusa, "Fluxgate can replace SQUID for lung diagnostics" in *Proc. of IEEE Sensors, 2002,* vol. 1, pp.321-324, 2002.

[12] K Tsukada and T. Kiwa, "Magnetic detecting device and material identiphying device" US Patent 7 525 308, 2009.

[13] M. P. Lecoeur, C. Fermon, H. Dyvorne, J.K. Jacquinot, H. Polovy and A.L. Walliang, „Magnetoresistive superconducting mixed sensors for biomagnetic applications", *JMMM,* vol 322, pp. 1647-1650, 2010.

[14] G. Bison, R. Wynands and A.Weis, „A laser-pumped magnetometer for the mapping of human cardiomagnetic fields", *Appl. Phys. B* vol. 76, pp. 325–328, 2003.

[15] M. Schmelz, R. Stolz, V. Zakosarenko, T. Schönau, S. Anders, L. Fritzsch, M. Mück and H. G. Meyer, „Field-stable SQUID magnetometer with sub-fT $Hz^{-1/2}$ resolution based on sub-micrometer cross-type Josephson tunnel junctions" *Supercond. Sci. Technol.* Vol. 6, 2011.

[16] S. Karsten and A. Braginski, Biomagnetism using SQUIDs status and perspectives", *Supercond. Sci. Technol.* vol. 19, pp. S160–S171, 2006.

[17] W. Andra and H. Nowak, *Magnetism in Medicine,* Ed.Weinheim, Wiley–VCH,1998.

[18] J. Clarke and A. I. Braginski, *SQUID Handbook vol I*, Ed. Berlin, Weinheim: Wiley–VCH, 2004.

[19] J. Clarke and A. I. Braginski, *SQUID Handbook vol II*, Ed. Berlin, Weinheim: Wiley–VCH, 2006.

[20] H. Weinstock, *SQUID Sensors: Fundamentals,Fabrication and Applications*,Ed. Dordrecht, Kluwer–Academic, 1995.

[21] J.P. Wikswo Jr, B.J. Roth, "The magnetic field of a single axon. A comparison of theory and experiment", *Biophisical Journal,* vol.48, pp.93-109, 1985.

[22] S. Sujit, "SQUID biosusceptometry in the measurement of hepatic iron", *Pediatr. Radiol*, vol. 33, pp.373-377, 2003.

[23] Y. Zheng, M. Saito, Y. Uchikawa and M. Kotani, "Research of laborer's magnetopneumography", *The Journal of the JBBS*, vol.13-1, pp.86-87, 2000.

[24] G. M. Brittenham, D. F. Farrel, J. W. Harris, E. S. Feldmann, E. H. Danish, W. A. Muir, J. H. Tripp and E. M. Bellon, "Magnetic susceptibility measurement of human iron stores", *N. Engl. J. Med.,* vol. 307, pp. 1671–1675, 1982.

[25] D. Paulson, R. L. Fagaly, R. M. Toussaint and R. Fischerm "Biomagnetic susceptometer with SQUID instrumentation", *IEEE Trans. Magn*. vol. 27, pp. 3249–3252, 1991.

[26] Magnetic declination, Available: http://magnetic-declination.com/.

[27] NOAA's Geophysical Data Center, Available: http://www.ngdc.noaa.gov/geomagmodels/struts/calcIGRFWMM.

[28] D. Costandache, A. Banarescu , O. Baltag, D. Zaharia and R. Ciorap "A complex installation for biomagnetism studies" in *Proc. World Congress on Medical Physics and Biomedical Engineering,* 2009, vol.25, pp. 556–558, 2009.

[29] M. Rau, O. Baltag, V. David, "Study of a mixed passive and active magnetic shielded room", in *Proc. International Conference on Electrical & Power Engineering,* Iasi, pp. 69-72, 2010.

[30] O. Baltag, O. Robu, D. Costandache, C. Ignat, *Magnetometrie,* Ed. Performantica, Iasi, 2003.

[31] O. Baltag, D. Costandache, A. Iftemie, M. Rau, I. Rau, S. Ojica, "Recording of the first magnetocardiogram in Romania", 12th International Balkan Workshop on Applied Physics, Constanta, Romania, 6-8 July 2011, unpublished.

Octavian Baltag was born in Bucharest, Romania on July 12, 1945. He graduated from Physics Faculty, Al.I.Cuza University of Iasi, Romania in 1971, and obtained his PhD in 1982.

From 1971 he was a researcher in the Institute of Technical Physics, Iasi. Since 2001 he was a professor at the Gr.T.Popa University of Medicine and Pharmacy Iasi, Romania, Faculty of Medical Bioengineering. He was a PhD Supervisor in Physics – Faculty of Physics, Al. I. Cuza Univ. of Iasi.

He is author of over 20 brevets of invention, 11 textbooks, over 350 papers. Current research interests are: high resolution magnetometry, bioengineering, microwaves applications in medicine, EMC.

Prof. Baltag earned more awards: the Henry Coanda Medal for inventor's activity, Traian Vuia Romanian Academy Prize, Romanian National Order of Merit, Knight Grade, and over 50 prizes from International Salon of Inventions and New Technologies.

Doina Costandache was born in Brasov, Romania, on August 20, 1951. She graduated the Physics Faculty, "Al. I. Cuza" University, Iasi, Romania in 1974 and obtained his PhD in 2009.

From 1978 she was a researcher in the Institute of Technical Physics, Iasi. Since 2000 and currently, she has been a lecturer, at the "Gr.T. Popa" University of Medicine and Pharmacy, Iasi, Faculty of Medical Bioengineering. She is author and coauthor of over 100 papers and 4 books. Current research interests are: high resolution magnetometry, bioelectromagnetism.

Ms Costandache is member of: IEEE, Romanian Society of Medical Bioengineering, and College of Medical Physicist in Romania. She received the Constantin Miculescu Romanian Academy Prize, 1981.

Miuta Carmina Rau was born in Tecuci, Romania, on March 3, 1969.

She graduated the Medical Bioengineering Faculty, in 2005, from "Gr. T. Popa" University of Medicine and Pharmacy, Iasi, Romania.

She is Ph. D. student at Faculty of Electrical Engineer, from "Gh. Asachi" Technical University of Iasi, Romania.

Current research interests are: Bioelectromagnetism, EMC.